SANDIA REPORT

SAND2005-4034
Unlimited Release
Printed July 2005

Final Test Results for the Schott HCE on a LS-2 Collector

Timothy A. Moss and Doug A. Brosseau

Prepared by Sandia National Laboratories
Albuquerque, New Mexico 87185 and Livermore, California 94550

Sandia is a multiprogram laboratory operated by Sandia Corporation,
a Lockheed Martin Company, for the United States Department of Energy's
National Nuclear Security Administration under Contract DE-AC04-94AL85000.

Sandia National Laboratories

Issued by Sandia National Laboratories, operated for the United States Department of Energy by Sandia Corporation.

Printed in the United States of America. This report has been reproduced directly from the best available copy.

Available to DOE and DOE contractors from
U.S. Department of Energy
Office of Scientific and Technical Information
P.O. Box 62
Oak Ridge, TN 37831

Telephone: (865)576-8401
Facsimile: (865)576-5728
E-Mail: reports@adonis.osti.gov
Online ordering: http://www.osti.gov/bridge

Available to the public from
U.S. Department of Commerce
National Technical Information Service
5285 Port Royal Rd
Springfield, VA 22161

Telephone: (800)553-6847
Facsimile: (703)605-6900
E-Mail: orders@ntis.fedworld.gov
Online order: http://www.ntis.gov/help/ordermethods.asp?loc=7-4-0#online

SAND2005-4034
Unlimited Release
Printed July 2005

Final Test Results for the Schott HCE on a LS-2 Collector

Timothy A. Moss, and Doug A. Brosseau
Solar Technologies
Sandia national laboratories
P.O. Box 5800
Albuquerque, NM 87185-1127

Abstract

Sandia National Laboratories has completed thermal performance testing on the Schott parabolic trough receiver using the LS-2 collector on the Sandia rotating platform at the National Solar Thermal Test Facility in Albuquerque, NM. This testing was funded as part of the US DOE Sun-Lab USA-Trough program. The receiver tested was a new Schott receiver, known as Heat Collector Elements (HCEs). Schott is a new manufacturer of trough HCEs. The Schott HCEs are 4m long; therefore, two were joined and mounted on the LS-2 collector module for the test. The Schott HCE design consists of a 70mm diameter high solar absorptance coated stainless steel (SS) tube encapsulated within a 125mm diameter Pyrex® glass tube with vacuum in the annulus formed between the SS and glass tube to minimize convection heat losses. The Schott HCE design is unique in two regards. First, the bellows used to compensate for the difference in thermal expansion between the metal and glass tube are inside the glass envelope rather than outside. Second, the composition of materials at the glass-to-metal seal has very similar thermal expansion coefficients making the joint less prone to breakage from thermal shock. Sandia National Laboratories provided both the azimuth and elevation collector module tracking systems used during the tests. The test results showed the efficiency of the Schott HCE to be very similar to current HCEs being manufactured by Solel. This testing provided performance verification for the use of Schott tubes with Solargenix trough collector assemblies at currently planned trough power plant projects in Arizona and Nevada.

Acknowledgements

We would like to acknowledge the fine work of Kye Chisman for cleaning up the wiring on the rotating platform. We would also like to thank Mike Edgar and Patricia Cordeiro for their work on the software for control and data acquisition, and Rod Mahoney for mentoring so we could get the best data possible.
Sandia is a multiprogram laboratory operated by Sandia Corporation, a Lockheed Martin Company, for the United States Department of Energy's National Nuclear Security Administration under contract DE-AC04-94AL85000.

Contents

Figures

Table

Final Test Results for the Schott HCE on a LS-2 Collector

Introduction

Sandia National Laboratories has completed thermal testing of a new Schott receiver on a LS-2 solar collector using the rotating platform at the NSTTF (National Solar Thermal Test Facility). The LS-2 is one of three generations of parabolic troughs manufactured by LUZ installed in the nine SEGS (Solar Electric Generating System) power plants in California. Together the nine plants produce about 360MW of electric power. The LS-2 design accounts for about 65% of the collectors installed.

Schott is a world leader in glass manufacturing and the receiver represents a new product for the company. Schott is now the second manufacturer of trough receivers, also known as HCEs (heat collecting elements), in the world. Previously, Solel was the only manufacturer of HCEs in the world. The Schott HCE design is interchangeable with the existing design. Schott has made some design changes in an effort to increase reliability and reduce the O&M costs associated with HCEs. They have matched the thermal expansion coefficients in the glass-to-metal seals, which are intended to reduce the vacuum leaks and glass breakages. The bellows between the metal tube and glass is inside the glass tube. The tube temperature will be about the same as the fluid temperature and the glass envelope temperature will be much lower due to the vacuum insulation between the two. As the fluid temperature increases the length of the tube will increase more than the glass and the bellows will compress, which slightly increases the surface area of the metal tube being heated by the concentrated sunlight. For the Solel HCEs the bellows is outside the glass tube and as the fluid temperature increases the bellows expand, which slightly decreases the surface area of the metal tube.

The Schott PTR 70 HCEs are 4 m long each; therefore two were joined together and mounted on the LS-2 collector. Figure 1 shows a picture of the LS-2 collector with the Schott HCEs on the rotating platform. The Schott HCE has a 70 mm diameter 316LSS tube with a high solar absorptance Cermet coating inside a 125 mm diameter Pyrex® glass tube. The space between the metal and glass tube is evacuated to minimize convection heat losses. An anti-reflection coating is applied to the inside and outside surfaces of the glass tube to increase transmittance through the glass. Schott claims their anti-reflective coating is more abrasion resistant than on existing HCEs, which should increase the lifetime of the coating when used in a solar plant.

Figure 1: Picture of the LS-2 concentrator with the Schott HCE on the rotating platform at the NSTTF. The top two rows of mirrors still have the early morning frost.

Background*:*

The LS-2 collector used at Sandia is the smallest portion of the complete solar collector assembly that can be operated independently and is also the largest collector that can be installed on the rotating platform. The collector has 20, thermally-sagged, second –surface silvered glass panels with a solar averaged specular reflectivity of 93 ±1.5% between different mirrors as well as between different areas of the same mirror. It has a 5 m aperture and a length of 7.8 m for an aperture area of 39.2 m^2. The LS-2 collector is designed for single axis tracking. This can subject the HCE to large solar beam incident angles and will significantly affect the efficiency of the HCE. If the collectors are mounted in a fixed east-west alignment of the trough rotational axis, zero incident angle occurs only at solar noon and is maximum at sunrise and sunset. If the trough rotational axis has some other orientation, such as north-south, a zero incident angel may not occur at all on some days of the year. The efficiency of the collector/HCE assembly is a function of the incident angle, called the incident angle modifier. Tests to determine the incident angle modifier for the Schott HCE were not done, by mutual agreement with all concerned parties, due to time constraints. The incident angel modifier for a LS-2 collector using a Luz Cermet HCE was determined and documented in a Sandia National Laboratories report[1], which is expected to be similar between the two HCEs. The test procedures used followed the ASHRAE[2] and ASTM[3] testing methodology for tracking concentrating solar collectors, except where noted in the SAND94-1884 document.

The LS-2 collector and Schott HCEs were performance tested for peak efficiency and for thermal heat loss. The thermal conversion efficiency at near ambient fluid temperatures, or optical efficiency, was measured using water. Using water at near ambient temperatures reduces the HCE thermal heat loss to almost zero, which gives the optimum thermal efficiency of the collector/HCE system. Equations for the properties of water were obtained by polynomial fits to data from NIST/ASME steam properties software[4]. Peak thermal conversion efficiency was also measured at elevated fluid temperatures, approaching 400˚C, using DOW Corning Syltherm® 800 as the HTF (heat transfer fluid). Equations for the properties of Syltherm® 800 were supplied by Dow Corning[5].

Peak thermal conversion efficiency is always conducted with a zero incidence angle and steady state conditions. For single axis tracking devices, like the LS-2, continuous zero incidence angle tracking is achieved by using the rotating platform for azimuth. The LS-2 elevation drive is used for elevation. Steady state conditions occur with zero incidence angle and constant HCE inlet and outlet fluid temperatures. Typical steady state conditions were established at 100˚C inlet temperature and then in 50˚C increments up to almost 400˚C.

Thermal heat loss tests as a function of HTF temperature were also conducted. Heat loss not only impacts measured peak collector module efficiency, but also heavily impacts plant operations with passing clouds. These tests are much more difficult to make since the ΔT across the HCE are about one order of magnitude less than the ΔT during peak efficiency testing while the measurement uncertainty remains the same. Heat loss testing is done on clear nights with winds less than 10 mph and the collector pointing straight up to maximize the radiant heat loss to deep space.

The flow rates through the HCE for testing on the rotating platform are about 55 l/min. This is much lower than 530 l/min used in the SEGS plants. To compensate for the lower flow rates a specially constructed plug is inserted down the full length of both Schott HCEs. The plug is made of a 50.8 mm diameter 304SS tube that has a 6.35 mm diameter 304SS tube spiral wound and tack welded along its perimeter. This gives an effective hydraulic diameter of 15.2 mm. The larger diameter tube is open at one end and closed at the other end with a 6.35 mm hole to remove any trapped air. Figure 2 shows a picture of the insert partially extracted from an HCE. The plug promotes turbulent flow of the fluid creating higher annular Reynolds numbers to simulate actual heat transfer coefficient in the SEGS at the lower flow rates. A detailed discussion of this is given in reference 1.

Figure 2: Picture of the insert used inside the HCE to increase turbulence in the fluid going through it.

Test Methodology

Thermal equilibrium must be established with the HTF in order to determine peak heat gain or loss during testing. Any fluid system can store thermal energy and the fluid system used with the
rotating platform is no exception. Without thermal equilibrium thermal energy can be either extracted or absorbed by the fluid system, which will add or subtract to the presumed thermal performance of the collector assembly. Thermal equilibrium is considered established during testing on the rotating platform when the HCE inlet and outlet fluid temperature vary less than ±0.2˚C over a minimum of 10 minutes. This is accomplished by first cooling the return flow from the HCE about 10 degrees below the desired inlet temperature and then heating to the determined inlet temperature using a PID controlled heater. The HCEs inlet and outlet temperatures were measured with a pair of RTDs with an accuracy of ±0.06˚C. When testing with water as the HTF, a pair of thermistors with an accuracy of ±0.02˚C is also used to measure the HCEs inlet and outlet temperatures.

Another important contributor to thermal equilibrium is achieving a stable flow rate. For this test the flow rate was stable to within ±0.1 l/min or better. The flowrate through the HCEs were measured with two turbine flowmeters calibrated to an accuracy of ±0.5% of reading between 0 and 15 gpm.

Wind speed has a secondary affect on thermal equilibrium, especially if it is gusting. Winds will vary the amount of heat being lost by the HCE and any piping used by the fluid loop. Winds can also cause the concentrator to wobble, which will cause the concentrator to slightly detrack in either azimuth and/or elevation. For this test the winds were 10 mph or less and not gusting. A P&ID of the fluid loop system used on the rotating platform is shown appendix A.

A constant energy input is also necessary for thermal equilibrium. The solar energy itself cannot be controlled, but the means to concentrate it can be. This is accomplished by tracking the sun as accurately as possible in azimuth and elevation and testing during clear sunny days one or two hours either side of solar noon when the atmospheric absorption is most constant. Sandia control software is capable of tracking the sun to ±0.09˚ in azimuth and ±0.08˚ in elevation. The solar energy input was measured with an Eppley NIP (Normal Incidence Pyrheliometer) calibrated to an accuracy of ±2% of reading. The NIP reading must be above 800 W/m^2 and vary less than 10% during the test period.

Mirror reflectivity changes will change the energy input to the HCE, but not in a manner to change thermal stability. During a test the reflectivity does not change, but it can change between tests such as being dustier after a windy day or cleaner after a rainstorm. The mirrors on the LS-2 collector were cleaned using de-ionized water to reduce any water spots and the glass specular reflectivity was measured before each test using a Devices & Services Co. reflectometer. The HCE glass is also cleaned to remove any soil and/or fingerprints from the glass using a clean soft towel and ethyl alcohol. Ethyl alcohol is used because it does not leave a residue when it dries.

The collector’s mirrors must be aligned so as to concentrate as much of the solar energy entering the collector’s aperture as possible onto the HCE in determining the peak thermal efficiency for a collector/HCE system. Mirror alignment itself does not affect thermal stability since any misalignment is constant, but it does impact the overall efficiency data. Documenting the mirror alignment does eliminate a source of variability when comparing these test results with other collector/HCE test results. A technique called the distant observer technique[6], adapted by Sandia and relatively new for trough testing, was used to measure the percent of mirror area that is aligned with the HCE. This technique assumes the sun is normal to the concentrator; any correction for off normal solar incidence is taken into account by the incident angle modifier. How this technique was applied to mirror alignment on the LS-2 is shown in Appendix B. For this test, the concentrator is pointed at an observer located about ¼ mile away. This is farther than the 0.11 mile distance calculated in Appendix B, which is the minimum distance. It is recommended to be at least twice the calculated minimum distance to ensure the observer is far enough to be equivalent to infinity for the concentrator. When the concentrator is pointed straight at the observer and the mirrors and HCE are perfectly aligned, the observer will see the HCEs black color completely fill the mirrors. Any mirror surface area that does not show black is not aligned with the HCE and, therefore will not concentrate the solar energy onto the HCE. Individual mirrors out of alignment are brought into alignment by adding or removing spacers placed between the mirror mounts and the mirror itself. Digital pictures are taken of the collector from this distant location. The percentage of mirror area out of alignment is calculated using the IMAC imagery software from National Instruments by comparing the number of black pixels to white pixels. There is no information on the average mirror alignment on currently installed trough systems.

Test Results

The mirrors on the LS-2 were aligned as best as possible to the Schott HCE using the distant observer technique. On-sun testing did not start until after the mirrors were aligned. A picture after the mirror alignment is shown in Figure 3. A before picture was not taken due to camera equipment problems. The IMAC imagery software determined about 10% of the available solar energy entering the aperture area was not focused on the HCE, which is any non-black area. The white vertical strip seen in Figure 3 was considered aligned even though it is white because it is actually the bellows shield cover where the two HCEs are joined together. This number does include the gaps between the mirrors, which accounts for approximately 2.5% of the total aperture area. The accuracy of this method is approximately ± 1%, which was determined by running the software several times using the same photo.

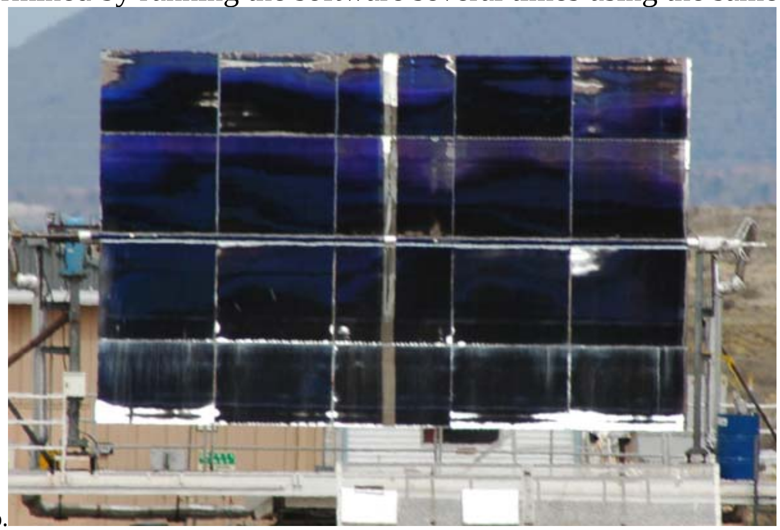

Figure 3: Picture of the mirror alignment of the LS-2 concentrator with the Schott HCE on the rotating platform, after the mirrors were aligned.

The data from each test for peak thermal conversion efficiency is shown in the Table 1 in Appendix C and is color coded to show the different stabilized inlet temperatures. The data acquisition system used LabVIEW version 7.01e. This software allows the user to set the resolution for the data collected or calculated and the values used for this test are also shown in appendix C. A plot showing the measured peak steady state thermal conversion efficiency vs. the average fluid temperature above ambient air temperature through the HCE is shown in Figure 4. The equation for the curve fit to the data is also shown in Figure 4. For comparison, the curve fit to the data collected from testing the LS-2 with a Luz Cermet HCE completed in 1994 is also shown in Figure 4. The efficiencies shown in Figure 4 were calculated based on a perfect mirror alignment, as recommended by ASHRAE[2] and ASTM[3]. This assumption was used for the earlier test done in 1994, but the actual alignment was not documented. This could cause some of the differences seen between the two sets of data. If the efficiencies were calculated using actual mirror alignment area then the efficiencies would be 10% higher because 10% is out of alignment.

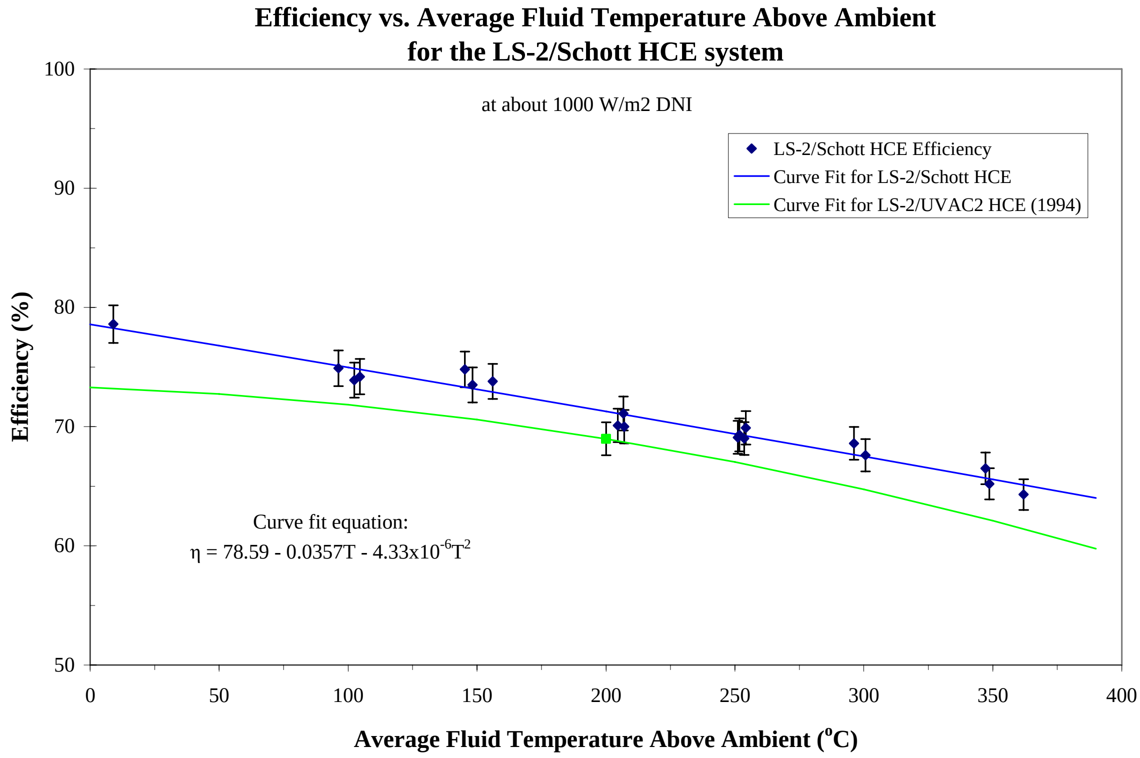

Figure 4: Plot of peak efficiencies vs. average HTF temperature through the HCE above ambient for the LS-2/Schott HCE test. Data from a previous test is also shown for comparison.

The measurement uncertainty of the data for this test, shown by the error bars in Figure 4, is about ±2.0%. The earlier test data measured uncertainty was also about ±2%, as shown by the one error bar shown in Figure 4 but holds throughout the temperature range. Appendix D shows how the errors were calculated for this test. A more detailed error analysis of testing on the rotating platform is given in reference 1. Statistically, there is little difference between the latest test data and the earlier test data, which is shown by the overlap of error bars in the plot, except at the lower temperatures. Both of these tests, however, did not take into account the uncertainty of the Syltherm® 800 properties since none could be obtained. The measured thermal heat loss vs. the average fluid temperature above ambient air temperature through the HCE is shown in Figure 5 for the LS-2/Schott HCE as well as the earlier test data for the LS-2/Cermet test for comparison. Data from the testing is shown in Table 2 in Appendix C. It should be noted that the surface area used for this data is the aperture area of the collector and not the absorber surface area, as recommended by ASHRAE[2] and ASTM[3]. The uncertainty of these measurements, as shown by the error bars in Figure 5, is about ± 5 W/m^2 vs. about ± 8 W/m^2 for the earlier test. These uncertainties are large because the measurements themselves are much smaller, ΔTs of about 0.5 vs. about 20˚C for efficiency testing, but the measurement error remains the same. Figure 5 shows the thermal loss for the LS-2/Schott HCE is lower than the previous test and the differences appear to be significant, as shown by the almost no overlap in error bars. These differences, however, could be explained by how the ΔTs were measured.

Past testing used matched pair type T thermocouples and for this testing RTDs were used. It is more difficult measuring a ΔT of 0.5˚C with matched pair type T thermocouples that are ± 0.2˚C accurate than using RTDs with an accuracy of ± 0.06˚C.

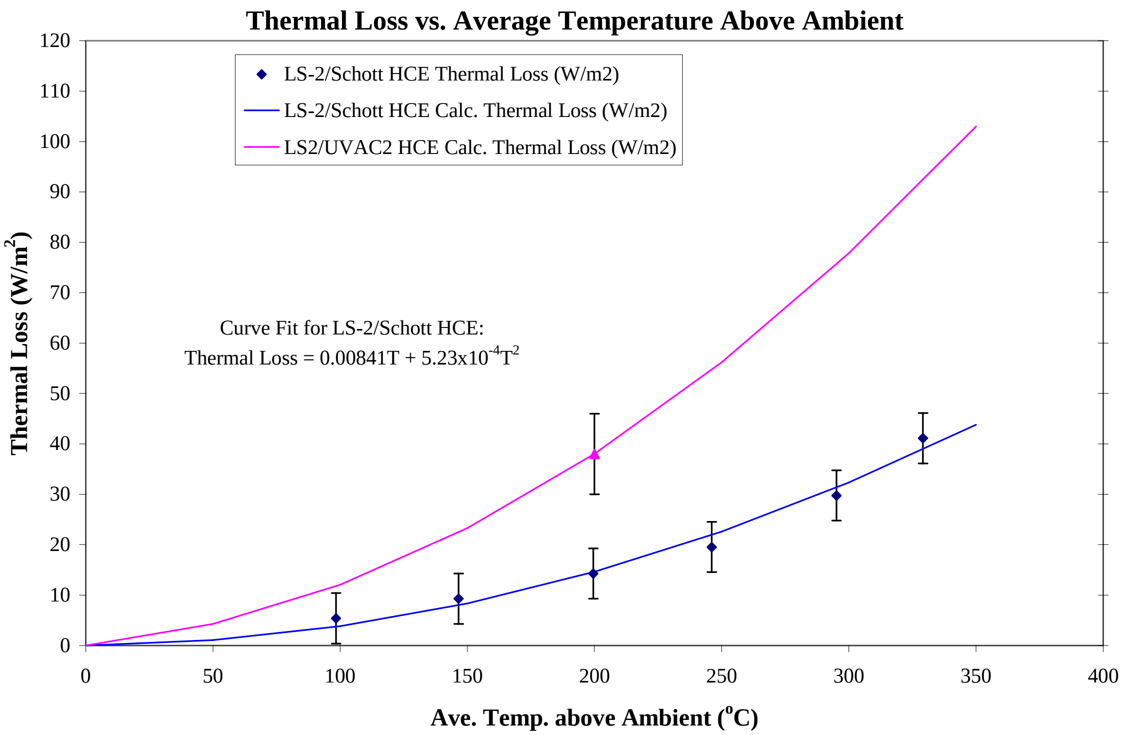

Figure 5: Plot showing the thermal loss for the LS-2/Schott HCE test at various temperatures. Data from a previous test is also shown for comparison.

References:

(1) V. E. Dudley, G. J. Kolb, M. Sloan, and D. Kearney, 1994, Sand94-1884, Test Results: SEGS LS-2 Solar Collector, Albuquerque, NM, Sandia National Laboratories

(2) ASHRAE – Methods of testing to Determine the Thermal Performace of Solar Collectors (ANSI approved), Standard 93-2003, 2003

(3) ASTM Standard E905-87(2001), Standard Test Method for Determining Thermal Performance of Tracking Concentrating Solar Collectors, 2001

(4) NIST Standard Reference Database 10, NIST/ASME Steam Properties, Version 2.21, May 2004

(5) Properties of Syltherm® 800 Heat Transfer Liquid, Midland, MI: Dow Corning Corporation, 1985

(6) R. L. Wood, 1981, UCRL-53220, Distant Observer Techniques for Verification of Solar Concentrator Optical Geometry, Livermore, CA, Lawrence Livermore National Laboratory

APPENDIX

Final Test Results for the Schott HCE on a LS-2 Collector

Appendix A - PI&D of the fluid loop

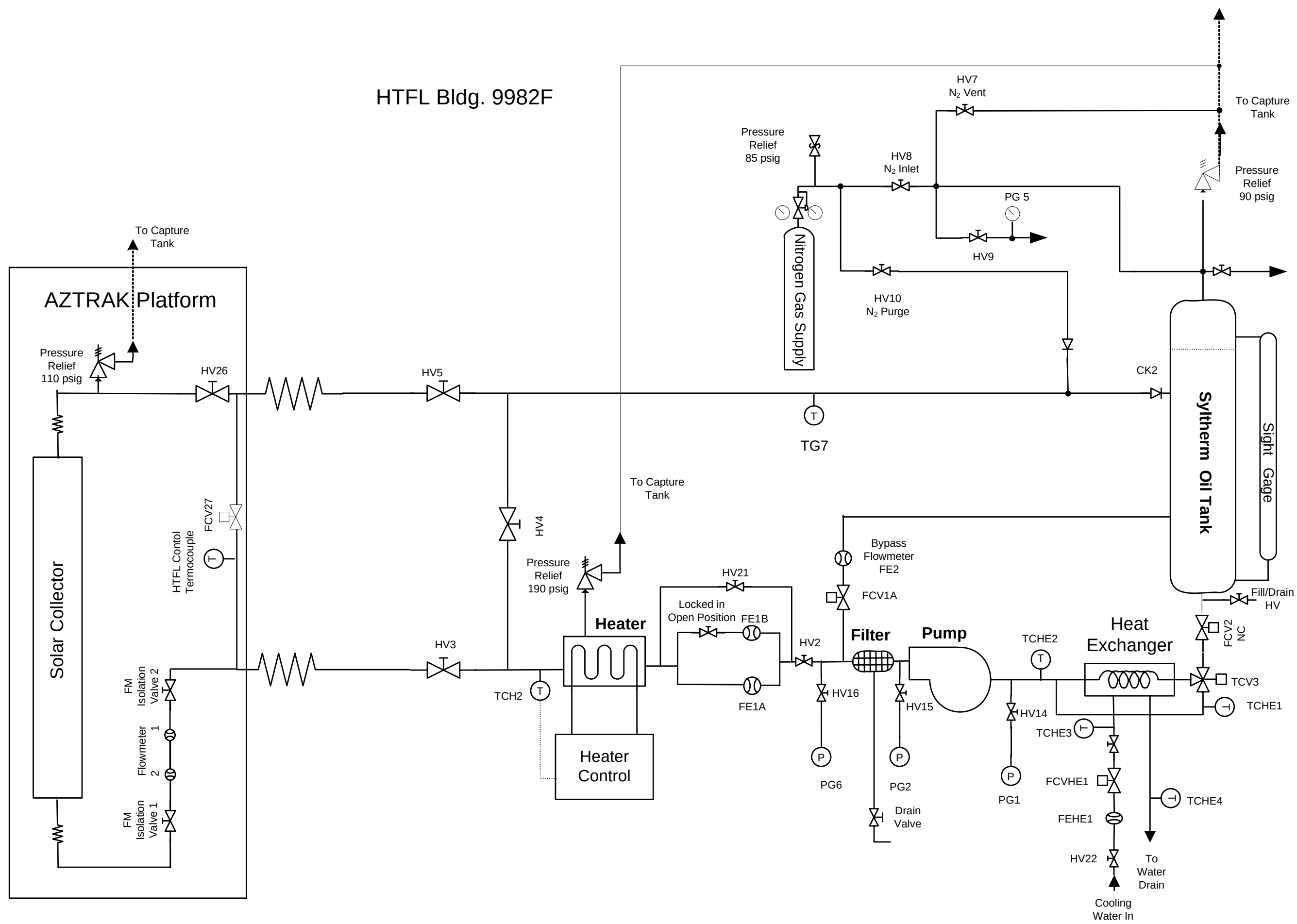

High Temperature Fluid Loop (HTFL) Schematic

TAM 8/2004

Appendix B - Estimating Minimum Distance Required for LS-2 Mirror Alignment Using the Distant Observer Technique

The LS-2 trough collector geometry:

Aperture: 5.0 m Focal Length: 1.49 m Absorber diameter: 0.070 m

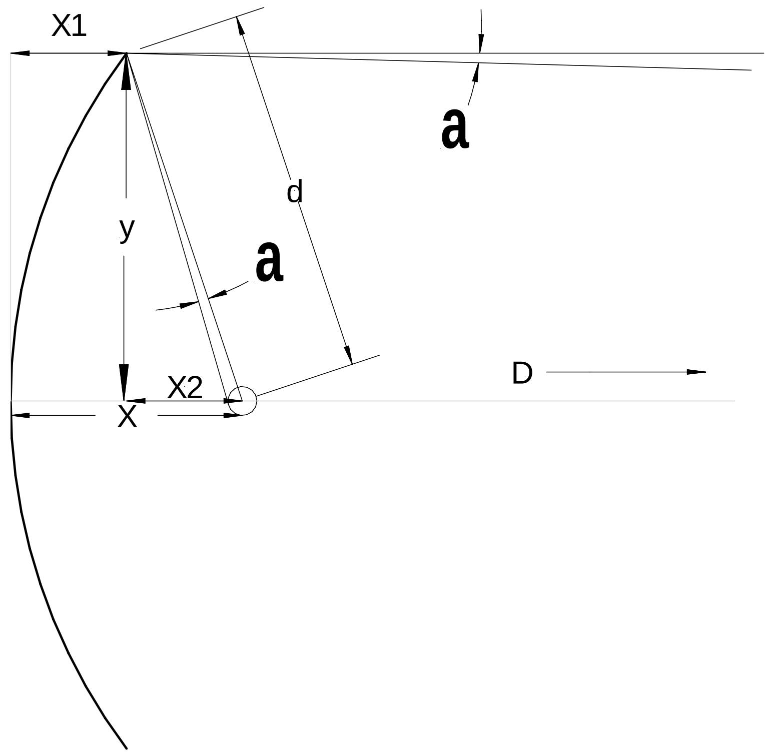

Using the formula for a parabola;

$$X1 = y^2/4f = (2.5)^2/4(1.49) = 1.05 \text{ m}$$

Now X = X1 + X2. To find X2 the equation becomes;

$$X2 = X - X1 = 1.49 - 1.05 = 0.44 \text{ m}$$

The distance from the mirror edge to the absorber center is:

$$d = (X2^2 + y^2)^{½} = (0.44^2 + 2.5^2)^{½} = 2.54 \text{ m}$$

α is the maximum parallax angle beyond which a distant viewer would not see the absorber tube with a perfect parabola and is defined as:

$\alpha \equiv$ the absorber radius/distance from the mirror edge to the absorber center

therefore; $\alpha = 0.035/2.54 = 0.014$ radians

D is defined as the distance at which a light ray that deviates from being parallel to the optical axis by α will cross the optical axis.

$$D = ½ \text{ aperture}/ \alpha = 2.5/0.014 = 178 \text{ m} = 0.11 \text{ miles}$$

Appendix C – Test Results

Table 1: Thermal Efficiency Test Data

Test Date	Average NIP	Average Ambient Air Temp	Average HTF Temp			Ave. HCE fluid Temp. Above Ambient	Average Flow Rate	Average Measured Efficiency		Ave. Wind Speed	
			Inlet	Outlet	ΔT						
CY2004	W/m^2	ºC	ºC	ºC	ºC	ºC	gal/min	%	± %	MPH	
10/19	999.45	17.98	21.35	33.13	11.78	9.26	9.95	78.6	2.00	4.5	water
12/14	985.01	5.60	70.57	91.26	20.69	75.32	14.27	72.8	1.59	3.3	70
12/20	985.92	6.37	70.40	92.23	21.83	74.95	13.89	73.7	1.59	6.31	
11/18	938.04	13.95	100.05	120.45	20.40	96.30	14.21	74.9	1.67	6.2	100
12/14	991.38	6.13	98.08	118.27	20.19	102.05	14.74	72.8	1.65	5.0	
12/17	1029.05	6.38	100.02	121.98	21.96	104.62	14.34	74.2	1.61	3.1	
12/20	1020.75	8.38	100.01	121.60	21.59	102.43	14.44	73.9	1.59	8.66	
11/18	943.47	14.67	150.00	169.89	19.89	145.28	14.72	74.8	1.64	4.1	150
12/10	934.30	13.44	151.76	171.61	19.85	148.25	14.35	73.5	1.62	5.9	
12/14	984.76	6.64	149.71	169.82	20.11	153.13	14.68	72.3	1.63	8.2	
12/17	1028.58	5.57	150.97	172.28	21.31	156.06	14.78	73.8	1.62	3.6	
12/2	1039.31	3.52	199.44	221.18	21.74	206.79	14.32	71.1	1.58	4.3	200
12/3	1051.08	5.83	199.56	221.28	21.72	204.59	14.27	70.1	1.56	5.3	
12/3	1044.73	4.83	201.13	222.62	21.49	207.05	14.33	70.0	1.53	6.2	
12/2	1035.56	5.76	249.19	270.84	21.65	254.26	14.42	69.9	1.58	3.5	250
12/3	990.35	8.37	248.81	269.46	20.65	250.77	14.31	69.2	1.52	5.7	
12/3	997.43	8.03	248.91	269.72	20.81	251.29	14.30	69.2	1.85	6.5	
12/3	1003.67	7.73	248.99	269.95	20.96	251.74	14.30	69.3	1.59	7.1	
12/3	1047.49	7.19	249.89	271.70	21.81	253.61	14.29	69.0	1.00	4.8	
12/2	953.29	7.63	298.27	318.20	19.93	300.61	14.45	67.6	1.59	3.0	300
12/10	971.46	12.38	298.16	318.92	20.76	296.16	14.34	68.6	1.51	10.1	
12/9	1004.64	11.56	347.76	369.67	21.91	347.16	14.41	66.5	1.50	13.8	350
12/10	1016.51	10.64	348.39	370.30	21.91	348.71	14.30	65.2	1.43	3.9	
12/10	1015.78	11.98	362.97	384.92	21.95	361.97	14.35	64.3	1.47	7.9	365

Table 1 showing the data collected during testing the Schott HCE on the LS-2 dish with color coding to show the different regions of stable temperature.

Table 2: Heat Loss Test Data

	Ave HCE Fluid Temp Above Ambient	ΔT Across HCE	LS-2/Schott HCE Thermal Loss (W/m^2)	thermal loss measurement error
Test Date	ºC	ºC	W/m^2	± W/m^2
12/13/2004	98.34	-0.15	5.38	4.25
12/13/2004	146.59	-0.27	9.28	4.36
12/13/2004	199.53	-0.41	14.28	4.26
12/14/2004	246.13	-0.58	19.53	4.09
12/14/2004	295.17	-0.90	29.77	4.09
12/14/2004	329.10	-1.29	41.13	3.89

Table 2 shows the data collected during thermal loss testing with the Schott HCE on the LS-2 dish.

Table 3: Data Ranges and Resolutions Used By LabVIEW version 7.01e

Tag Name	Item	Raw Full Scale	Raw Zero Scale	Eng Full Scale	Eng Zero Scale	Units	Log Resolution (eng units)
XCPC Main Control In (deg C)	Ch 101	100	0	100	0	deg C	0.01
LS2 TC1 Tmp In (V)	Ch 109	21	0	21	0	mV	0
LS2 TC1 Tmp Out (V)	Ch 110	21	0	21	0	mV	0
DNI (W|m^2)	Ch 300	0.00835	0	1000	0	W/m^2	0
Wind Speed (mph)	Ch 303	5	0	100	0	mph	0
Wind Direction (V)	Ch 304	10	0	10	0	Volts	0
Coll Flow 1 (V)	Ch 305	10	0	10	0	Volts	0
Coll Flow 2 (V)	Ch 306	10	0	10	0	Volts	0
HTFL Flow Hi (gpm)	Ch 307	10	0	10	0	gpm	0.1
HTFL Flow Lo (gpm)	Ch 308	10	0	10	0	gpm	0.1
Wtr Oil Test (V)	Ch 315	100	0	100	0	Volts	0.1
LS2 RTD1 Tmp In (ohm)	Ch 600	250	100	250	100	ohms	0
LS2 RTD1 Tmp Out (ohm)	Ch 601	250	100	250	100	ohms	0
LS2 Therm1 Tmp In (ohm)	Ch 602	12000	1100	12000	1100	ohms	0
LS2 Therm1 Tmp Out (ohm)	Ch 603	12000	1100	12000	1100	ohms	0
LS2 RTD2 Tmp In (ohm)	Ch 604	250	100	250	100	ohms	0.1
LS2 RTD2 Tmp Out (ohm)	Ch 605	250	100	250	100	ohms	0.1
Ambient Temp (ohm)	Ch 606	100	0	100	0	ohms	0.1
AZTRK Az (bin)	Ch 700	100	0	100	0		0
Type T Ref T HP3852 Slot 100	REFT 100	100	0	100	0	deg C	0
LS2 RTD1 Eff (%)		100	0	100	0	%	0.01
LS2 RTD2 Eff (%)		100	0	100	0	%	0.01
LS2 TC1 Eff (%)		100	0	100	0	%	0.01
LS2 Enthalpy Eff(%)		100	0	100	0	%	0.01
Wind Direction (deg)		360	0	360	0	deg	0.1
AZTRK Az (deg)		360	0	360	0	deg	0.01
Solar El (deg)		90	0	90	0	deg	0.01
Solar Az (deg)		360	0	360	0	deg	0.01
LS2 RTD1 Tmp Delta (deg C)		100	0	100	0	deg C	0.01
LS2 RTD2 Tmp Delta (deg C)		100	0	100	0	deg C	0.01
LS2 RTD1 Tmp Ave (deg C)		100	0	100	0	deg C	0.01
LS2 RTD2 Tmp Ave (deg C)		100	0	100	0	deg C	0.01
LS2 TC1 Tmp Delta (deg C)		100	0	100	0	deg C	0.01
LS2 TC1 Tmp Ave (deg C)		100	0	100	0	deg C	0.01
LS2 RTD1 Tmp Out (deg C)		100	0	100	0	deg C	0.01
LS2 RTD1 Tmp In (deg C)		100	0	100	0	deg C	0.01
LS2 RTD2 Tmp Out (deg C)		100	0	100	0	deg C	0.01
LS2 RTD2 Tmp In (deg C)		100	0	100	0	deg C	0.01
LS2 TC1 Tmp Out (deg C)		100	0	100	0	deg C	0.01
LS2 TC1 Tmp In (deg C)		100	0	100	0	deg C	0.01
LS2 RTD1 Av Abv Amb (deg C)		100	0	100	0	deg C	0.01
LS2 RTD2 Av Abv Amb (deg		100	0	100	0	deg C	0.01

C)							
LS2 TC1 Av Abv Amb (deg C)		100	0	100	0	deg C	0.01
Coll Flow 2 (gpm)		15	0	15	0	gpm	0.01
Coll Flow 1 (gpm)		15	0	15	0	gpm	0.01
LS2 RTD1 Cp (J|kg deg C)		100	0	100	0	J/kg deg C	0.01
LS2 RTD2 Cp (J|kg deg C)		100	0	100	0	J/kg deg C	0.01
LS2 TC1 Cp (J|kg deg C)		100	0	100	0	J/kg deg C	0.01
LS2 MFL (kg|hr)		100	0	100	0	kg/hr	0.01
LS2 RTD1 Enpy Out (kJ|kg)		100	0	100	0	kJ/kg	0.01
LS2 RTD1 Enpy In (kJ|kg)		100	0	100	0	kJ/kg	0.01
LS2 RTD2 Enpy Out (kJ|kg)		100	0	100	0	kJ/kg	0.01
LS2 RTD2 Enpy In (kJ|kg)		100	0	100	0	kJ/kg	0.01
LS2 TC1 Enpy Out (kJ|kg)		100	0	100	0	kJ/kg	0.01
LS2 TC1 Enpy In (kJ|kg)		100	0	100	0	kJ/kg	0.01
LS2 RTD1 Ht Gain (kW)		100	0	100	0	kW	0.01
LS2 RTD2 Ht Gain (kW)		100	0	100	0	kW	0.01
LS2 TC1 Ht Gain (kW)		100	0	100	0	kW	0.01
LS2 Power In (kW)		100	0	100	0	kW	0.01
LS2 Meas Col Ap (m^2)		100	0	100	0	m^2	0.001
LS2 RTD1 Visc (N sec|m^2)		0.001	0	0.001	0	N sec/m^2	0
LS2 RTD2 Visc (N sec|m^2)		0.001	0	0.001	0	N sec/m^2	0
LS2 TC1 Visc (N sec|m^2)		0.001	0	0.001	0	N sec/m^2	0
LS2 RTD1 Reynolds #		100	0	100	0		0.1
LS2 RTD2 Reynolds #		100	0	100	0		0.1
LS2 TC1 Reynolds #		100	0	100	0		0.1
LS2 Therm1 Av Abv Amb (deg C)		100	0	100	0	deg C	0.01
LS2 Therm1 Cp (J|kg deg C)		100	0	100	0	J/kg deg C	0.01
LS2 Therm1 Eff (%)		100	0	100	0	%	0.01
LS2 Therm1 Enpy In (kJ|kg)		100	0	100	0	kJ/kg	0.01
LS2 Therm1 Enpy Out (kJ|kg)		100	0	100	0	kJ/kg	0.01
LS2 Therm1 Ht Gain (kW)		100	0	100	0	kW	0.01
LS2 Therm1 Reynolds #		100	0	100	0		0.1
LS2 Therm1 Tmp Ave (deg C)		100	0	100	0	deg C	0.01
LS2 Therm1 Tmp Delta (deg C)		100	0	100	0	deg C	0.01
LS2 Therm1 Visc (N sec|m^2)		0.001	0	0.001	0	N sec/m^2	0
LS2 Therm1 Tmp In (deg C)		100	0	100	0	deg C	0
LS2 Therm1 Tmp Out (deg C)		100	0	100	0	deg C	0
Ambient Temp (deg C)		100	0	100	0		0.01

Appendix D – Error Analysis

In calculating the error in any measurement two sources must be accounted for; systematic and random errors. Systematic error is the error of the instrument used to make the measurement. Random error is the data scatter from making the same measurement more than once.

For this test the sources of and the values used for systematic errors are:

Temperature	RTDs for average fluid temperatures through the HCE	±0.06 ˚C
	Type T for ambient air temperature	±0.5 ˚C
	Thermistors for average water temperature through HCE	±0.06 ˚C
	$\Delta T = \sqrt{2} * (\text{RTD error})^2$ for oil	±0.12 ˚C
	$\Delta T = \sqrt{(\text{RTD})^2 + (\text{thermistor error})^2}$ for water	±0.12 ˚C
Flow rate		±0.05%
Solar insolation		±2.0%

The random errors used for this test are the scatter in the data during a period of stabile temperatures, flow rates, and solar insolation. The random error for the calculated values of heat gain, or loss, specific heat, fluid density, and efficiency are calculated using the root-sum-square method defined as:

$$E_{rss} = \sqrt{[\Delta u_1(\partial F/\partial u_1)]^2 + [\Delta u_2(\partial F/\partial u_2)]^2 + \quad + [\Delta u_n(\partial F/\partial u_n)]^2}$$

The equation for heat gain (or loss) is:

Q = flow rate * fluid density * fluid specific heat * temperature change

$$\text{Or } Q = f * \rho * C_p * \Delta T$$

The equation for calculating the density of the heat transfer fluid:

$$\rho = a + bT + cT^2 + dT^3$$

where:	for water (g/m^3)	for oil (kg/m^3)
a =	.99987	953.16027
b =	$7.10307\text{x}10^{-5}$	$-9.16442\text{x}10^{-1}$
c =	$8.40755\text{x}10^{-6}$	$4.20074\text{x}10^{-4}$
d =	$4.78384\text{x}10^{-8}$	$-1.66873\text{x}10^{-6}$

The equation for calculating specific heat of the heat transfer fluid:

$$C_p = a + bT + cT^2 + dT^3 \text{ in kJ/kg/˚C}$$

where:	for water	for oil
a =	4.21699	1.57418
b =	$-2.92000\text{x}10^{-3}$	.00171
c =	$7.46237\text{x}10^{-5}$	$4.20074\text{x}10^{-4}$
d =	$-6.3777\text{x}10^{-7}$	

For heat gain, Q, the error equation is:

$$E_Q = \sqrt{[E\rho(\partial Q/\partial \rho)]^2 + [E_{\Delta T}(\partial Q/\partial \Delta T)]^2 + [E_f(\partial Q/\partial f)]^2 + [E_{Cp}(\partial Q/\partial_{Cp})]^2}$$

Where:

$\partial Q/\partial \rho$	=	$f * C_p * \Delta T$
$\partial Q/\partial \Delta T$	=	$f * \rho * C_p$
$\partial Q/\partial f$	=	$\rho * C_p * \Delta T$
$\partial Q/\partial Cp$	=	$f * \rho * \Delta T$
$E\rho$	=	$E_T * \partial \rho/\partial T$
$E_{\Delta T}$	=	ΔT measurement error, ˚C
E_f	=	flow measurement error, m^3/sec
E_{Cp}	=	$Et * \partial C_p/\partial T$

E_T	=	temperature measurement error, ˚C
$\partial\rho/\partial T$	=	$b + 2cT + 3bT^2$
$\partial C_p/\partial T$	=	$b + 2cT$ for oil and $b + 2cT + 3dT^2$ for water
ρ	=	fluid density, kg/m^3
Q	=	heat gain (loss), W
f	=	fluid flow, m^3/sec
C_p	=	fluid specific heat, kJ/kg/˚C
T	=	average fluid temperature through the HCE, ˚C
ΔT	=	fluid temperature change across the HCE, ˚C

The equation for deriving the efficiency is:

$$\eta = \text{heat gain/heat input} = Q / (\text{solar insolation} * \text{collector aperture})$$

where: the collector aperture is $39.2m^2$

The error equation for efficiency is:

$$E_\eta = \sqrt{[E_Q(\partial\eta/\partial Q)]^2 + E_i(\partial\eta/\partial i)]^2}$$

Where:

E_Q	=	error in heat gain
E_i	=	error in solar insolation
$\partial\eta/\partial Q$	=	1/(insolation * aperture)
$\partial\eta/\partial i$	=	-Q/(insolation^2 *aperture)

An example is shown below for the test run on November 18, 2004 with a stable inlet temperature of 100˚C.

Inlet	100.05 ± .0202˚C
Outlet	120.45 ± .0902˚C
ΔT	20.40 ± .0925˚C
Ambient air	13.95 ± .2157˚C
Flow rate	$8.963 \times 10^{-4} \pm 1.306 \times 10^{-6}$ m^3/sec
Density	854.991 ± 0.0818 kg/m^3
Specific heat	1762.30 ± 0.1580 J/kg/˚C
Insolation	938.04 ± 3.67 W/m^2
Heat gain	702.77 W/m^2
$\partial Q/\partial\rho$	32.22
$\partial Q/\partial\Delta T$	1350.47
$\partial Q/\partial f$	30736585
$\partial Q/\partial C_p$	15.362
$E\rho$	-0.5122 kg/m^3
$E_{\Delta T}$	0.1515 ˚C
E_f	4.668×10^{-6} m^3/sec
E_{Cp}	0.98898 J/kg/˚C
E_T	0.5790 ˚C
$\partial\rho/\partial T$	-0.885
$\partial C_p/\partial T$	1.708
E_Q	6.401 W/m^2
η	74.92%
$\partial\eta/\partial Q$	1.066x10-^{3}
$\partial\eta/\partial I$	-7.987x10-^{4}

Using the above numbers, the error in the efficiency, E_η = 1.67%

Distribution List

Mark Mehos 3
Hank Price
Al Lewandowski
National Renewable Energy Laboratory
1617 Cole Blvd.
Branch 4710/115
Golden, CO 80401-3393

Gilbert Cohen 1
Solargenix
2101-115 Westinghouse Blvd
Raleigh, NC 27604

Bob Cable 1
Solargenix Energy
P.O. Box 1621
Helendale, CA 92342

Randy C. Gee 1
Solargenix Energy
13991 West 54th Avenue
Arvada, CO 80002

Scott Canada 1
APS Solar Services
400 North 5th Street, M.S. 4160
Phoenix, AZ 85004

Dr. Thomas Kuckelkorn 1
Schott-Rohrglas
Abt. SR/ES
Erich Schott-Str. 14
95666, Mitterteich

Dr. Alex Marker 1
Schott North America, Inc.
Regional Research and Development
400 York Avenue
Duryea, PA 18642-2036

Dr. Nikolaus Benz 3
Schott-Rohrglas GmbH
Erich-Schott-Strasse 14
P.O. Box 1180
95660 Mitterteich
Germany

Frank (Tex) Wilkins 1
U.S. Department of Energy EE-2A
Office of Solar Energy Technologies
1000 Independence Avenue, SW
Washington, DC 20585

Tommy Rueckert 1
U.S. Department of Energy EE-2A
Concentrating Solar Power
1000 Independence Avenue, SW
Washington, DC 20585

MS 0703 J. Nelson, 6218 1
MS 1127 T. Mancini, 6218 1
MS 9018 Central Technical Files, 8945-1
MS 0899 Technical Library, 9616 1